

Characterization of Mo Deposited on a TiO₂(110) Surface by Scanning Tunneling Microscopy and Auger Electron Spectroscopy

András Berkó,* Anett Magony, and János Szökő

Department of Solid State and Radiochemistry and Reaction Kinetics Research Group of the Hungarian Academy of Sciences, University of Szeged, P.O. Box 168, H-6701 Szeged, Hungary

Received December 21, 2004

The properties of Mo ultrathin films deposited on a TiO₂(110) surface were investigated by scanning tunneling microscopy (STM) and spectroscopy (STS), as well as by Auger electron spectroscopy (AES). The substrate exhibited mainly large (1 × 1) terraces decorated by additional [001] rows (missing or added 1D structures) of reduced TiO_x phases. Only a few percent of the surface exhibited a cross-linked (1 × 2) arrangement. The deposition of Mo layers at room temperature with a rate of approximately 0.4 monolayer/min resulted in nanoclusters of 1–2 nm with a low-profile shape (2D-like). Preferential decoration of the atomic steps was not found; at the same time, the 1D defect sites of missing or added rows on the (110) terraces were characteristically decorated by larger Mo nanocrystallites. This behavior indicates that the mobility of Mo atoms is higher on the more reduced regions of the substrate. The high dispersion of the Mo adlayer changed only slightly on annealing up to 700 K; in the range of 900–1050 K, however, a significant increase of the particle size accompanied by splitting of the TiO₂(110) terraces was observed. This behavior may be explained by the partial oxidation of the supported Mo (accompanied by the reduction of the substrate) into tetragonal crystallites oriented and slightly elongated in the [001] or [110] direction of the TiO₂(110) support. STS measurements indicated that the crystallites or the support/crystallite interface formed above 900 K possesses a wide band gap. The annealing above 1050 K resulted in the disappearance of Mo from the TiO₂(110) surface, which may be explained by the formation and sublimation of MoO₃ species at the perimeter of the nanoparticles. The change of AES signal intensities for O(KLL) and Mo(MNN) as a function of the annealing temperature also supports this mechanism.

1. Introduction

The catalytic behavior of VB–VIIB metals (such as W, Mo, and Ta) and their compounds (oxide, carbide, nitride, sulfide) in nanocrystallite and nanocluster form have received a great deal of attention in both fundamental and applied research.^{1–3} The supported nanoparticles of these materials may play an important role in the development of new catalysts for hydrocarbon conversion and pharmaceutical chemistry, and they may also constitute key components of gas sensors fabricated by nanotechnological methods.

To learn fine details about the chemical properties of the isolated nanoparticles (metal, oxide, etc.) and their interactions with the support and the surrounding gases, the fabrication and the study of so-called 2D (planar) systems recently became a research field of great relevance. For this purpose the application of scanning tunneling microscopy (STM) is especially useful, since the active sites of the model catalysts can be imaged in a very high lateral resolution.⁴ To achieve this goal, it is naturally very important that the 2D model systems fabricated by the different methods should exhibit the active sites in a high surface concentration. In the last 10–15 years the techniques for the preparation of this type of materials

have been thoroughly elaborated. The most frequently applied method is the metal vapor deposition (MVD) of the catalytic metals onto the surface of oxide single crystals.^{5,6} The metal nanoparticles so formed are frequently very reactive, which opens the way for the fabrication of nanoparticles of their compounds (oxide, carbide, sulfide) too.

Turning our attention to a more specified material system, namely, oxide-supported Mo, MoO_x, and Mo_xC nanoparticles, it can be established that only a few works—especially STM studies—were presented in this field.^{7–14} Most of these works deal with the deposition of Mo on TiO₂ single-crystal surfaces. Mo belongs to the so-called reactive deposits which react easily with the bulk oxygen of the reducible oxides. The crucial issues connected to this topic are the following: (i) the role of the MoO_x interface in forming a thicker Mo film, (ii) the structural identification of the Mo–MoO_x nanocrystallites, and (iii) the influence of the deposition rate of Mo on the oxidation

* To whom correspondence should be addressed. Phone: +36 62 544 646. Fax: +36 62 420 678. E-mail: aberko@chem.u-szeged.hu.

(1) Oyama, S. T. In *The Chemistry of Transition Metal Carbides and Nitrides*; Oyama, S. T., Ed.; Blackie Academic and Professional: Glasgow, Scotland, 1996; p 1.

(2) Solymosi, F.; Németh, R.; Széchenyi, A. *Catal. Lett.* **2002**, *82* (3–4), 213.

(3) Topsøe, H.; Clausen, B. S.; Massoth, F. E. *Hydrotreating Catalysis, Science and Technology*; Springer: Berlin, 1996; see also references therein.

(4) Bäumer, M.; Freund, H.-J. *Prog. Surf. Sci.* **1999**, *61*, 127.

(5) Campbell, C. T. *Surf. Sci. Rep.* **1997**, *27*, 1.

(6) Henry, C. R. *Surf. Sci. Rep.* **1998**, *31*, 231.

(7) Kitchin, J. R.; Barteau, M. A.; Chen, J. G. *Surf. Sci.* **2003**, *526*, 323.

(8) Chun, W.-J.; Asakura, K.; Iwasawa, Y. *Chem. Phys. Lett.* **1998**, *288*, 868.

(9) Domenichini, B.; Pétigny, S.; Blondeau-Patissier, V.; Steinbrunn, A.; Bourgeois, S. *Surf. Sci.* **2000**, *468*, 192.

(10) Blondeau-Patissier, V.; Lian, G. D.; Domenichini, B.; Steinbrunn, A.; Bourgeois, S.; Dickey, E. C. *Surf. Sci.* **2002**, *506*, 119.

(11) Domenichini, B.; Blondeau-Patissier, V.; Casanove, M. J.; Lian, G. D.; Bourgeois, S. *J. Cryst. Growth* **2004**, *263*, 256.

(12) Domenichini, B.; Petukhov, M.; Rizzi, G. A.; Sambì, M.; Bourgeois, S.; Granozzi, G. *Surf. Sci.* **2003**, *544*, 135.

(13) Blondeau-Patissier, V.; Domenichini, B.; Steinbrunn, A.; Bourgeois, S. *Appl. Surf. Sci.* **2001**, *175–176*, 674.

(14) Pétigny, S.; Domenichini, B.; Mostéfa-Sba, H.; Lesniewska, E.; Steinbrunn, A.; Bourgeois, S. *Appl. Surf. Sci.* **1999**, *142*, 114.

state of the surface or, in other words, the kinetics of the surface diffusion and the surface reduction–oxidation processes. It is clear from earlier studies that the resistance of Mo nanoclusters to sintering is probably connected with the high activity of Mo toward surface oxygen.^{7,8,12} This behavior is also revealed in the sensitivity of the growing mode of Mo ultrathin layers (at least in the initial stage) for the stoichiometry of the TiO₂ surfaces.^{9,10,14} Because of the competitive effects of the kinetics of the surface diffusion of Mo atoms and the reaction with the surface oxygen, the deposition rate and the temperature also determine very sensitively the formation of a MoO_x interface.^{7,12}

In this work a detailed STM–Auger electron spectroscopy (AES) study is presented on the characteristic morphological features of the formation of Mo ultrathin layers on a TiO₂(110)-(1 × 1) surface decorated by 1D defect structures.

2. Experimental Section

The experiments were carried out in an ultra-high-vacuum (UHV) chamber equipped with a room temperature scanning tunneling microscope (WA-Technology), a cylindrical mirror analyzer (STAIB) applied for AES, and a quadrupole mass spectrometer (Balzers) for gas analysis.

A TiO₂(110) single crystal of 5 × 5 × 1 mm³ was stuck with oxide adhesive (Ceramabond-571, Aremco Products) to a Ta filament and mounted onto a transferable sample holder. The probe was heated ohmically by flowing current through the Ta filament. The temperature of the sample was measured by a chromel–alumel thermocouple stuck onto the TiO₂ sample also by Ceramabond-571. A typical cleaning procedure consisted of several cycles of 5 min of Ar⁺ bombardment (1.5 keV, 10⁻⁵ A cm⁻²) and 10 min of annealing at 1100 K in a UHV. From time to time the surface was reoxidized in oxygen (10⁻⁴ Pa) at 800 K.

The cleanliness of the sample and the metal overlayer was checked by Auger electron spectroscopy. The Mo coverage is expressed in monolayer equivalents (ML), which corresponds to approximately 1.5 × 10¹⁵ atoms cm⁻². For the estimation of the actual coverage, both the first break point of the absolute intensity of the characteristic AES signal of Mo as a function of deposition time and the total volume of the nanoparticles determined on the basis of STM images were taken into account. The relative duration of the deposition was used for the estimation of other coverages.¹⁵ The error of the coverage determined by this method was estimated to be less than 15–20%.

W-tips fabricated electrochemically in KOH solution were used for STM imaging, and they were sharpened “in situ” above the TiO₂ surface by applying 5–10 V pulses. In accordance with this procedure, it seems to be very probable that the imaging atom at the end of the tip can be either an O or a Ti atom. If it is not mentioned otherwise, the tunneling parameters of +1.5 V and 0.2 nA are typically set for imaging.

Mo was deposited by a commercial MVD source (Oxford Applied Research) equipped with a high-purity Mo rod (99.95%). The typical deposition rate of 0.4 ML min⁻¹ was used throughout this work. The sample–source distance was chosen to be 10 cm for the elimination of radiative heating of the sample by the source cooled by flowing water.

3. Results

3.1. Characterization of the TiO₂(110) Substrate Applied in This Work. The atomic-scale morphology of TiO₂(110) surfaces has been described in detail in numerous works (refs 16–23 and references therein). It was

shown that a large variety of characteristic surface features can appear depending on the pretreatment and the past of the crystals. Accordingly, it is worth presenting the actual morphology of the TiO₂(110) surface applied for further studies in this work.

The most important large-scale features are the atomic terraces of 100 nm on average separated mainly by [001] steps as can be seen on an area of 200 nm × 200 nm (Figure 1A). These steps are regularly decorated by much shorter [110] and [111] steps of 3–10 nm size. If these steps are more extended, the surface exhibits (1 × 2) reconstruction, although in our case this latter feature was spread over only a few percent of the total surface. The wide (1 × 1) terraces showed additional 1D strands running in the direction of [001] and 0D dots distributed randomly on the surface as can be seen in the images of 50 nm × 50 nm (Figure 1B,D). The interstrand area was identified as a bulk-terminated 1 × 1 arrangement depicted by the STM image of 10 nm × 10 nm (Figure 1C). The light rows are attributed to 5-fold Ti⁴⁺ sites separated by 0.65 nm.²¹ At the middle bottom of this image an outlying 1D strand can also be found. It is important to remark that basically two different 1D strands can be distinguished: a shorter/brighter one (BS) and a longer/darker one (DS) with an average length of 15–20 and 50–100 nm, respectively (Figure 1B,D). The identification of the BS and DS structures grown on the top of the (1 × 1) surface is rather controversial.^{16–23} This issue has recently received renewed attention.^{22,23} Takakusagi et al. have rendered the BS structures to Ti₂O₃ rows and the DS form to Ti₃O₅ added rows;²² in contrast to this, Bennett and co-workers identified the BS stripes as Ti₃O₅ added rows, although they did not explain the inner structure of the DS stripes.²³

Our experimental data revealed that the imaging nature of the longer/darker 1D strands (DS) exhibits a rather surprising behavior depending on the state of the tip. In the case of the contrast experienced most often (tip state I)—as was described above—the long 1D strands show a brightness of middle level relative to the well outlying shorter 1D strands (BS), which exhibit usually lighting dots at their ends (Figure 1D,G). In the case of a slightly modified state of the imaging tip (tip state II), both types of 1D strands split into double rows, as shown in Figure 1E,H. This is a transition state to the best resolution state (tip state III) where the Ti⁴⁺ rows of the 1 × 1 arrangement are very intensively visible; at the same time, the longer 1D strands (DS) appear as deep dark rows and the shorter ones display a weakly outlying character (Figure 1F,I). It should be mentioned that the inner part of the 1 × 1 arrangement also exhibits dark and short 1D islands. These latter features may be identified with some contamination adsorbed on the Ti⁴⁺ sites or with missing Ti⁴⁺ sites (Figure 1I). It was experienced many times that the abrupt alteration of the imaging from tip state I into state III is strictly connected with the alteration of the chemical state of the end of the tip (probably caused by the change of the imaging atom), and it cannot simply be explained by the change of the imaging current or bias. It should be mentioned that all of the images presented in Figure 1 were recorded with $U_{\text{bias}} = +1.5$ V and $I_t = 0.2$ nA. In accordance with our experiences, the imaging ability

(15) Berkó, A.; Ménesi, G.; Solymosi, F. *Surf. Sci.* **1997**, *372*, 202.

(16) Diebold, U. *Surf. Sci. Rep.* **2003**, *48*, 53.

(17) Fischer, S.; Munz, A. W.; Schierbaum, K.-D.; Göpel, W. *Surf. Sci.* **1995**, *337*, 17.

(18) Cocks, I. D.; Guo, Q.; Williams, E. M. *Surf. Sci.* **1997**, *390*, 119.

(19) Tanner, R. E.; Castell, M. R.; Briggs, G. A. D. *Surf. Sci.* **1998**, *412/413*, 672.

(20) Li, M.; Hebenstreit, W.; Gross, L.; Diebold, U.; Henderson, M. A.; Jennison, D. R.; Schultz, P. A.; Sears, M. P. *Surf. Sci.* **1999**, *437*, 173.

(21) Onishi, H.; Iwasawa, Y. *Surf. Sci.* **1999**, *313*, L783.

(22) Takakusagi, S.; Fukui, K.-I.; Nariyuki, F.; Iwasawa, Y. *Surf. Sci.* **2003**, *523*, L41.

(23) Bennett, R. A.; Stone, P.; Price, N. J.; Bowker, M. *Phys. Rev. Lett.* **1999**, *82* (19), 3831.

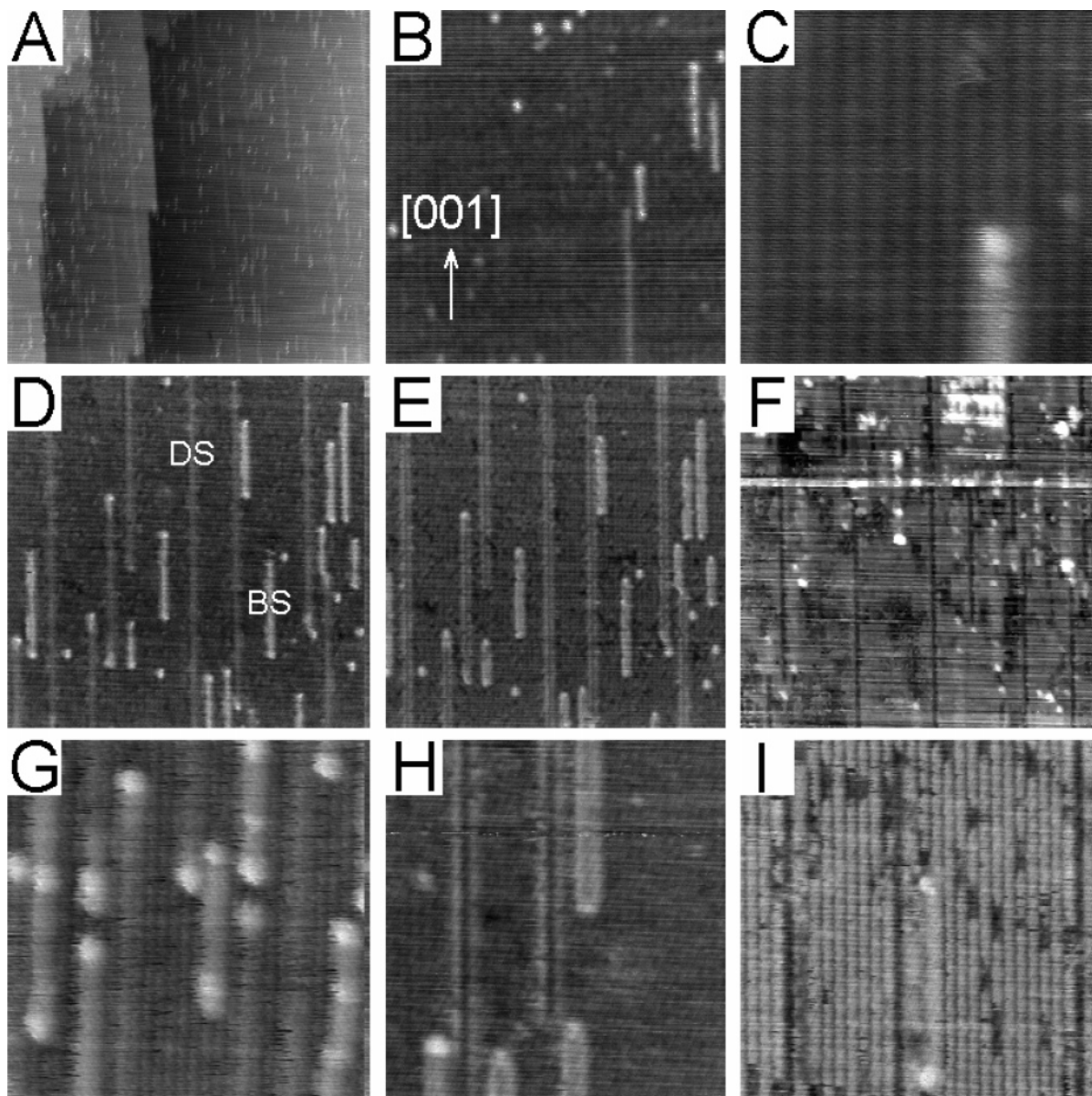


Figure 1. Characteristic STM images of different scales recorded on a clean $\text{TiO}_2(110)$ surface: (A) $200 \text{ nm} \times 200 \text{ nm}$; (B) $50 \text{ nm} \times 50 \text{ nm}$; (C) $10 \text{ nm} \times 10 \text{ nm}$. Effect of the change of the tip: (D, G) tip state I; (E, H) tip state II; (F, I) tip state III. Size of the latter images: (D–F) $50 \text{ nm} \times 50 \text{ nm}$; (G–I) $20 \text{ nm} \times 20 \text{ nm}$.

predominating in Figure 1D,G can be more easily achieved than tip state III of the best resolution shown in Figure 1F,I. In other words, tip state I is much more stable than tip state III. It can be assumed that the apex atom of the tip is mostly a W atom, although tip regeneration (bias pulses) can result in an apex atom of Ti or O. In the latter case, probably a tiny TiO_x adparticle forms on the tip. To clear this question, a theoretical STM simulation is needed; nevertheless, the large difference between the stabilities of the tip states makes it very probable that the tip apex is the W atom in state I and the Ti ion in tip state III.

As the structure of the $\text{TiO}_2(110)$ support, the axis of the long dark rows (DS) fits well to the periodicity of (1×1) light rows (Figure 1I). It is worth noting that the neighboring light rows exhibit a slightly increased height caused certainly by a modified tunneling probability in the vicinity of DS structures (Figure 1I). This phenomenon can well be the cause of the appearance of the double outrising structure seen in tip state II (Figure 1H). On the basis of the argumentation above, the dark strands (DS) may be identified as missing TiO_x rows, where x can be more than 2. It can be assumed that the 5-fold Ti^{4+} row

and the neighboring in-plane O rows are missing and the next-neighboring bridging O rows relax toward the nanopit formed in this way. This relaxation causes probably the slightly enhanced tunneling ability of the neighboring light rows (Figure 1H,I).

To our best knowledge, the systematic transformation (described above) from the more easily achieved imaging state to the best resolution imaging has not been published yet (Figure 1G,H,I). In contrast to the previous identifications of this structure, we suggest that the darker strands (DS) cannot be a geometrically outrising feature but rather a 1D defect (missing) site of the (1×1) surface. Taking into account that the BS features are substantially different both from the DS features and from the outrising rows of the 1×2 arrangement, the BS stripes may be identified as defect added rows of Ti_3O_5 . Regarding the main surface features of $\text{TiO}_2(110)$ presented above, it can be concluded that both 1D structures (BS and DS) constitute reduced regions of the surface.

3.2. Deposition of Mo onto the $\text{TiO}_2(110)$ Surface at Room Temperature. The deposition of Mo on the clean $\text{TiO}_2(110)$ was monitored by AES and STM at 300

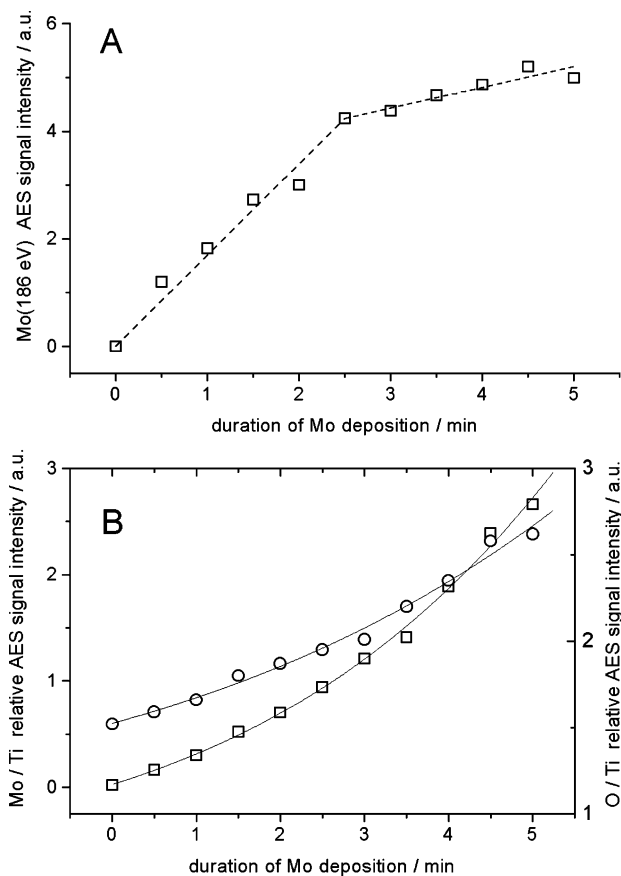


Figure 2. Change of (A) the absolute intensity of the Mo (186 eV) AES signal and (B) that of the relative AES signals of Mo ($R_{\text{Mo}} = I_{\text{Mo}(186 \text{ eV})}/I_{\text{Ti}(385 \text{ eV})}$) and of O ($R_{\text{O}} = I_{\text{O}(510 \text{ eV})}/I_{\text{Ti}(385 \text{ eV})}$) as a function of the duration of Mo deposition.

K. In Figure 2A the change of the absolute intensity of the Mo(LLM) Auger signal appearing at 186 eV is plotted as a function of duration. It can be seen that the intensity of the AES signal of Mo increases linearly with two different slopes in the range of 0–2.5 and 2.5–5.0 min, respectively. The clear change of the slope at 2.5 min indicates a Stransky–Krastanov growing mode (2D first layer) of Mo. It is worth mentioning that the intensity of the AES signal became constant (or slightly decreased) by extending the deposition period for more than 5 min. This result suggests (and will be supported by the STM measurements; see below) that the completion of the first Mo monolayer takes place after approximately 2.5 min under our deposition conditions. It is important to mention that during this experiment the performance of the AES spectrometer was kept rigorously constant in terms of e-beam intensity, multiplayer voltage, and position of the probe. On the basis of these experimental data, the relative AES signals (R_{Mo}) calculated for Mo (186 eV) and Ti (385 eV) peak intensities (Mo/Ti) were also plotted versus duration (Figure 2B). In this case, the ratio increased rather continuously with only a very faint indication of some breaking points. It can be seen that the relative AES ratio is approximately $R_{\text{Mo}} = 0.90$ for the surface covered by 1 monolayer (ML) of Mo at 300 K, while this value is 2.70 for 2 MLs. A very similar curve was obtained for the O (510 eV)/Ti (385 eV) ratio (R_{O}) (Figure 2B). Surprisingly, the relative AES signal for oxygen also intensified with the increase of the Mo coverage. This feature can be explained by different processes: (i) preferential shadowing of the Ti sites of the surface by the Mo deposits; (ii) induced segregation of subsurface oxygen into the Mo ultrathin layer; (iii) some contamina-

tion of the deposited Mo layer by oxygen-containing adsorbates. It should be mentioned that some carbon contamination was detected above 1–2 MLs of Mo coverage. In the case of a Mo-free TiO₂(110) surface, the value of $R_{\text{O}} = 1.45$ was measured; for Mo coverages of 1 and 2 MLs this value increased to 1.85 and 2.65, respectively. Taking into account the XPS and XPD results obtained by Domenichini et al. for the same system,¹² we tend to assume that the Mo overlayer becomes partially saturated with oxygen already at 300 K (case ii above).

Figure 3A–C shows STM images of 20 nm × 20 nm recorded on the TiO₂(110) surface covered by Mo in different amounts (0.02, 0.10, and 1.0 ML) at room temperature. The first image (A) exhibits lines characteristic of the original (1 × 1) pattern of the support; moreover, a 1D outlying strand in the middle part of the image and some Mo nanoparticles of approximately 1 nm formed on the TiO₂(110)-(1 × 1) terraces. By increasing the Mo coverage, the size of the supported Mo nanoparticles gradually increased to 2 nm (Figure 3B,C). The last image of this series exhibits a strand outlying in the middle part of the picture containing the largest particles. These STM results suggest that Mo covers the TiO₂(110) surface in a rather high dispersity with clear evidence for the formation of 2D-like low-profile shape particles at 300 K.

To obtain more detailed information on the early stage of Mo deposition (0.02 ML), images of 20 nm × 20 nm were taken in different regions of the surface (Figure 3D–F). In the flat (1 × 1) terraces decorated by BS and DS structures the larger admetal particles consisting of approximately 10–15 atoms are selectively bonded to these 1D features (indicated by arrows), although the (1 × 1) regions also exhibit localization of smaller crystallites. The appearance of the larger (probably 3D) nanoparticles with a height of 0.4–0.5 nm on the BS and DS structures does not mean that the admetal is bonded more strongly in these regions of the surface. On the contrary, the accumulation of the deposited Mo atoms into larger particles suggests that the activation barrier of the surface diffusion of Mo atoms is smaller along the DS and BS regions. This behavior is also manifested in the appearance of larger crystallites on the (1 × 1) terraces after a gentle annealing of a Mo-deposited (a few percent of a monolayer) surface (see below). By analyzing the position of the small dots in the (1 × 1) textured region, it can be concluded that the nanoparticles appearing after Mo deposition (probably identifiable with Mo nanoparticles) are not preferentially located on the 5-fold Ti⁴⁺ sites (light rows) (Figure 3D,E). A region with an atomic step of [001] can be identified in image E. It is clearly seen that the step is also not selectively decorated by larger Mo nanoparticles, although a single middle-sized particle is located in the line of the step. The decoration of the DS region (in the middle of the image) is also a relevant morphological feature in this case (Figure 3E). The next image depicts a 20 nm × 20 nm area and exhibits a region of a cross-linked (1 × 2) reconstruction (Figure 3F), where Mo particles are selectively sitting on the outlying rows of a more reduced Ti₂O₃ stoichiometry.

3.3. Effects of Annealing on Mo-Deposited TiO₂(110) Surfaces. Figure 4 shows the change of relative AES signals ((A) R_{Mo} , (B) R_{O}) on the effect of annealing the Mo-deposited TiO₂(110) surface for two different initial metal coverages. The relative AES signal (R_{Mo}) decreased in the temperature range of 300–700 K, and then it increased slightly up to 900 K followed by a rather sharp decrease up to 1100 K (Figure 4A). In these measurements, the surface was consecutively annealed at the tempera-

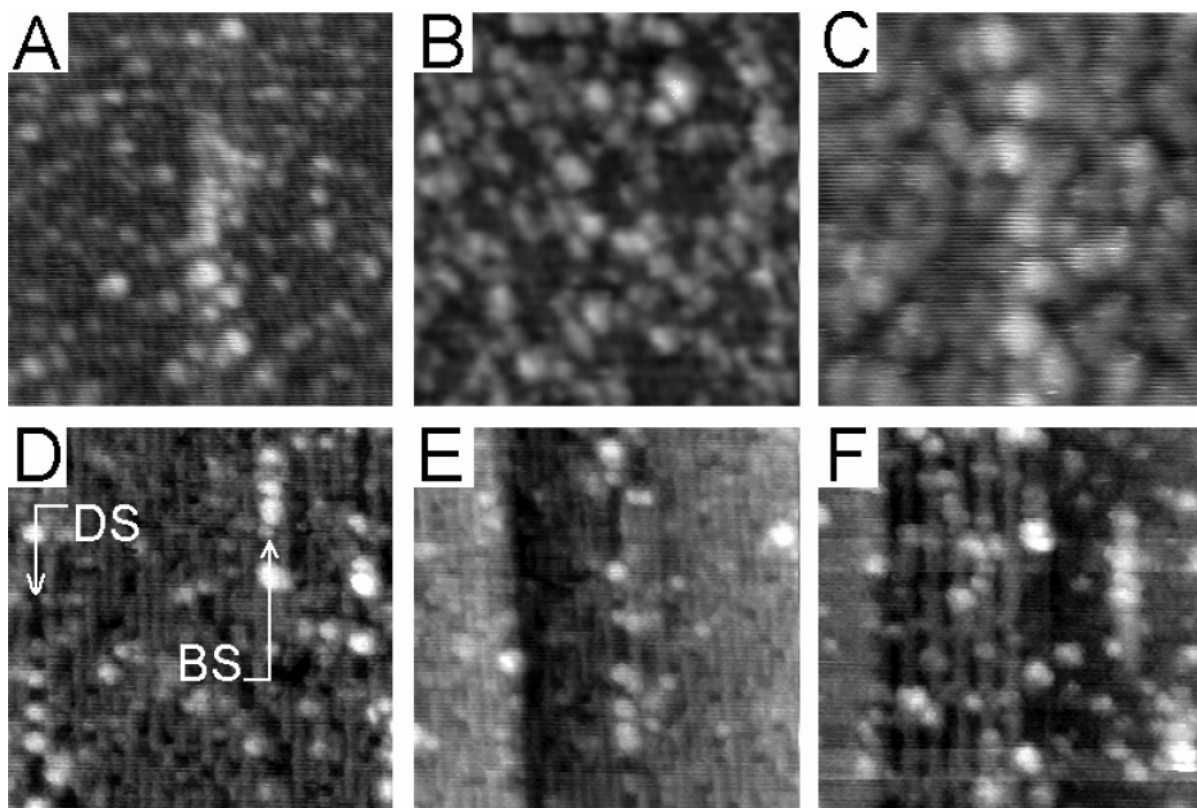


Figure 3. STM images of $20 \text{ nm} \times 20 \text{ nm}$ detected for Mo/TiO₂(110) surfaces of different admetal coverages: (A) 0.02 ML; (B) 0.10 ML; (C) 1.0 ML. (D–F) STM images ($20 \text{ nm} \times 20 \text{ nm}$) of different regions of the TiO₂(110) surface covered by approximately 0.02 ML of Mo.

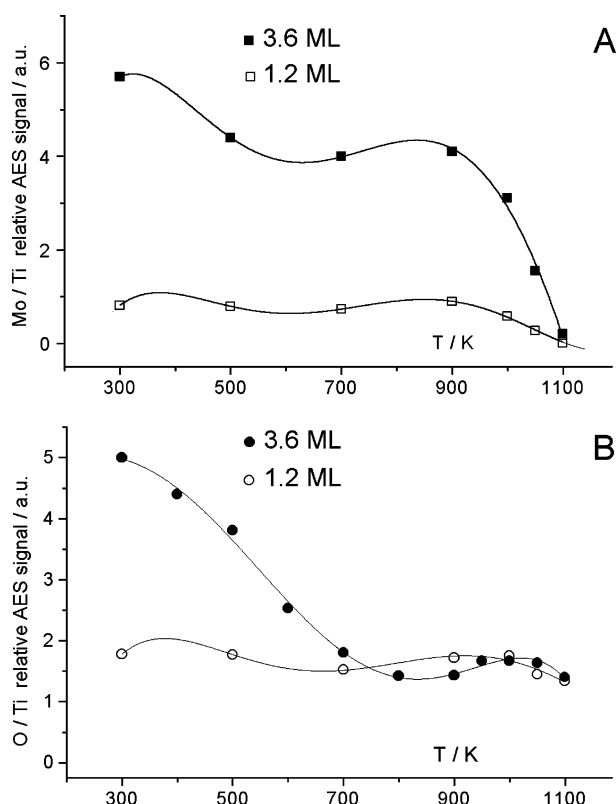


Figure 4. Effect of successive 2 min annealing of Mo-deposited samples on the relative intensity (A) of the Mo signal (R_{Mo}) and (B) of the O signal (R_{O}) for two different initial coverages of the admetal.

tures indicated on the curve for 2 min. AES spectra were recorded after cooling of the samples back to room

temperature. The change of the relative AES signal for oxygen (R_{O}) exhibits a behavior similar to that for Mo: a decrease up to 700–800 K and a moderate increase in the range of 800–1000 K, followed by a drop back to the value characteristic of the clean oxide surface (approximately 1.45) in the range of 1000–1100 K.

The effect of annealing on the transformation of the characteristic morphology of the surface containing different amounts of deposited Mo was also systematically investigated. The STM images ($50 \text{ nm} \times 50 \text{ nm}$) taken in these experiments are collected in Figure 5. Three different initial Mo coverages were studied which were determined from the relative AES signal intensity of Mo measured at 300 K (see Figure 2), and the duration of the deposition was also taken into account. In the case of the smallest coverage (0.09 ML) a single (1×1) terrace can be seen where the regions of the 1D bright strands (BS) are decorated by the largest nanoparticles, while the (1×1) terrace regions exhibit somewhat smaller adparticles (Figure 5A). With the increase of the initial coverage, the contrast of the BS features merges into the contrast of the adparticles sitting on terraces, while the average size of the Mo nanoparticles gradually grows: 1.8 and 2.9 nm for 1.2 and 3.6 MLs, respectively. Annealing at 500 and 700 K does not result in a noticeable change of the surface texture at higher coverages, although an increase in the average size of the particles can be clearly observed for 0.09 ML (Figure 5B). In this latter case, mainly the smallest particles (or adatoms) existing on the (1×1) terraces are sintering into larger ones, resulting in the weakening contrast of the DS and BS features. It is worth noting that even in this case the particles have low shape 2D character. The step line occurring in the middle of the image (700 K, 0.09 ML) does not show any special accumulation of Mo particles. Much more perceptible

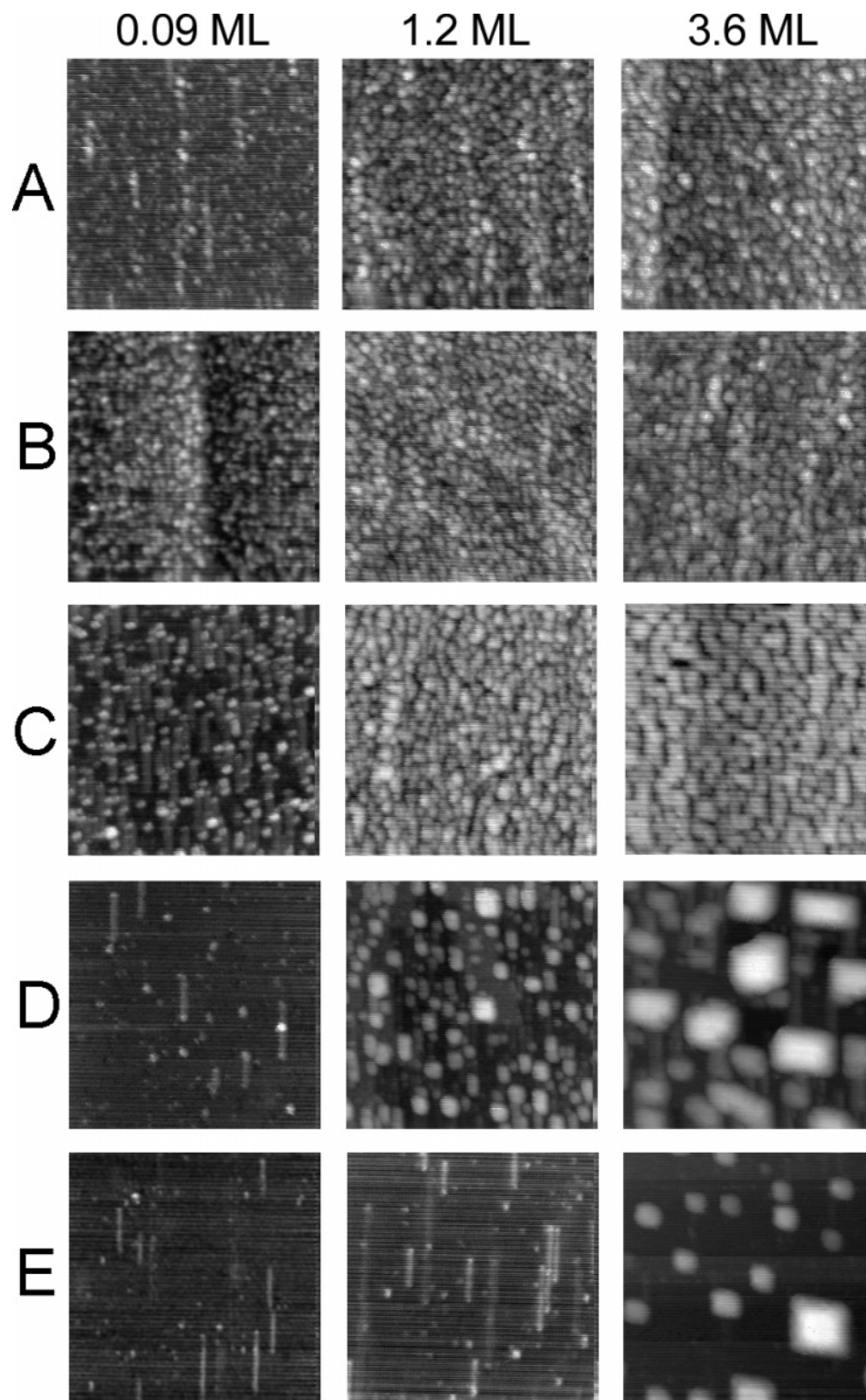


Figure 5. Characteristic STM images taken on Mo/ $\text{TiO}_2(110)$ samples: Mo deposited at room temperature (A) and annealed for 2 min at higher temperatures of (B) 700 K, (C) 900 K, (D) 1050 K, and (E) 1100 K in the case of three different initial Mo coverages (0.09, 1.2, and 3.6 MLs). Size of the images: 50 nm \times 50 nm.

changes occurred after the thermal treatment at 900 K for 2 min (Figure 5C). The main feature is the ordering of the particles in the directions of [001] and $[\bar{1}10]$ and also some increase in the average size of the nanoparticles. At the lowest coverage (0.09 ML) outrising 1D stripes are formed, and they are typically decorated by particles on their ends. The formation of the particles in rectangular shape is well observable for 3.6 ML coverage. Nevertheless, the average corrugation of the surface did not change

significantly in these treatments; the values were 0.6–0.9 nm at 700 K and 0.7–1.2 nm at 900 K. In contrast to this, the annealing at 1050 K resulted in a pronounced alteration of the morphology (Figure 5D). In the case of the lowest coverage the surface became free of adparticles; only the outrising 1D strands and some 0D dots can be seen on the image (1050 K, 0.09 ML). For the coverage of 1.2 MLs, the size distribution of the nanoparticles became rather wide. The terraces of the support are split by

irregular step lines, and the middle-sized particles exhibit some elongation in the direction of [001]. The edges of the largest rectangular particles of 4–5 nm size are clearly directed toward the main crystallographic orientation of the $\text{TiO}_2(110)$ support. In the case of the largest Mo coverage (3.6 MLs), annealing at 1050 K results in a few very large particles of 8–10 nm with elongation in the direction of [110], besides a lot of smaller nanoparticles. In this latter case, the corrugation of the detected area was more than 3 nm. The very wide size distribution of the adparticles may indicate that the compositions of the smaller and the larger particles are different. It can be supposed that the tiny particles contain more oxygen (they are more oxidized) and the larger ones are more metallic, especially the top layers of them. In the case of 1.2 ML coverage, the effect of further annealing at 1100 K resulted in the recreation of the clean $\text{TiO}_2(110)$ surface decorated with BS and DS structures. However, this change is not completed for a 3.6 ML initial Mo coverage, although the thermal treatment resulted also in a dramatic decrease in the total volume (by a factor of approximately 5) and in a significant change of the distribution of the crystallites. Moreover, the shape of the crystallites became completely rectangular. AES measurements showed that after a more extended annealing at 1100 K the adparticles can entirely be removed even at this high initial coverage.

Considering the calibration of the amount of Mo admetal, it is very important to mention that the calculation of the total volume of Mo nanoparticles was applied for calibration of the coverage. For this purpose the particles that were clearly distinguishable on a surface heated to 900–1000 K were taken into account. The results obtained in this way have shown a fine correlation between the first breaking point of the absolute AES intensity of Mo plotted as a function of deposition time (see above in Figure 2) and the total volume expected for approximately 1 ML of Mo. It must naturally be assumed that the accuracy of this type of calibrations cannot be better than 15–20%.

In parallel experiments the characteristic I – V curves (scanning tunneling spectroscopy (STS)) were also detected on the top of the adparticles at the different stages of the annealing. It was supposed that the local spectroscopy of the particles provides information about the oxidation state of individual nanoparticles. The results are presented in Figure 6 for the annealing of the surface covered by 3.6 MLs of Mo. The I – V curve taken at room temperature on an outrising particle (indicated by a circle in the 20 nm \times 20 nm image) shows quasi ohmic character with some oscillating behavior. This latter property may be connected with some unordered structure at the particle/support interface, resulting in upcharging and decharging effects. After the annealing of the surface at 500 and 700 K, the I – V curve recorded on the top of a crystallite (indicated on the STM image) also shows ohmic behavior. This statement is also valid for the sample annealed at 900 K. Some weakening of the ohmic character is measured after the treatment at 1000 K, as can be seen in Figure 6. In this latter case the slope of the I – V curve decreased strongly at the Fermi level. After the subsequent annealing at 1050 K the I – V spectrum reveals an insulator character of the particle: the slope at the Fermi level is close to zero, and the width of this region (band gap) is approximately 2.5 eV. From these results it can be concluded that the Mo deposit displays near-metallic character up to 900 K; the thermal treatments above this temperature result in particles exhibiting insulator characteristics. It is important to note that this behavior can be explained in several different ways: (i) the particle became totally

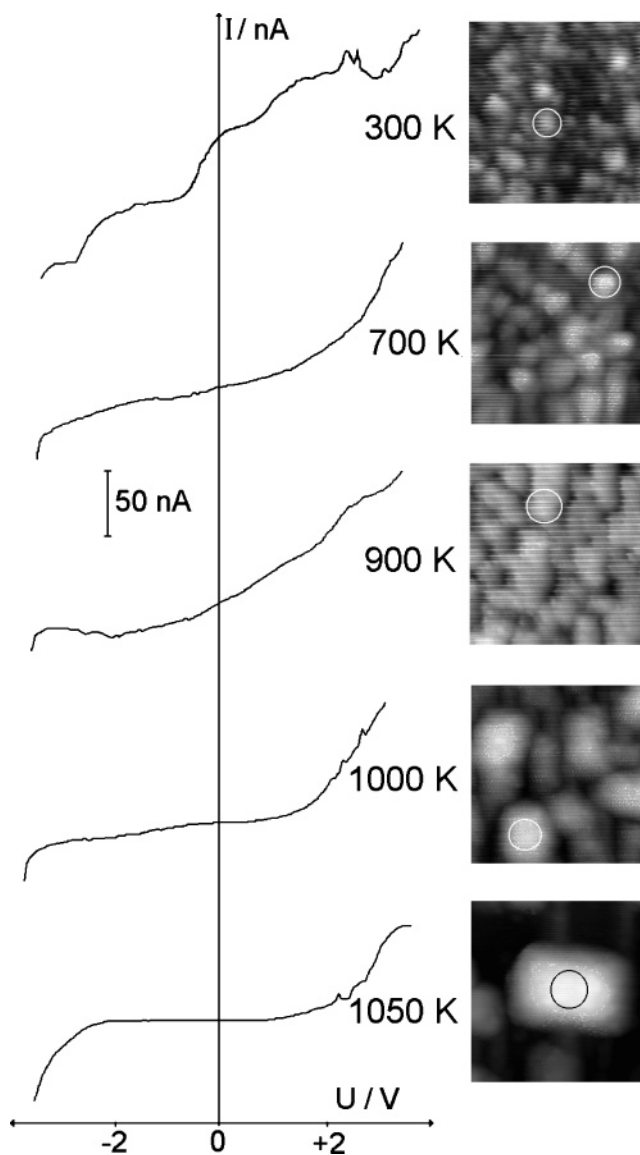


Figure 6. I – V spectra recorded in the middle point of the nanoparticles (indicated by circles) formed by deposition of 3.6 MLs of Mo on a $\text{TiO}_2(110)$ surface at 300 K followed by annealing for 2 min at higher temperatures.

oxidized; (ii) an interface of a well-ordered oxide between the particle and the substrate was formed; (iii) the particle was covered by a thin oxide layer of the support (encapsulation). From the STS measurement alone it is difficult to determine the mechanism playing the main role in the phenomenon. The particle encapsulation is an important effect for supported noble metals (Pt, Rh), as was demonstrated in an earlier paper,²⁴ and the study of the epitaxial growing of TiO_x on the $\text{Mo}(110)$ surface has also shown a high wetness ability of the oxide layer on the supporting metal surface.²⁵ The bulk oxidation of the large particles may be excluded on the basis of thermodynamic data.⁷ Accordingly, the most probable mechanism is the formation of a well-ordered oxide interface between the particle and the substrate, although the encapsulation of Mo particles by the TiO_x layer cannot be completely excluded. An atomically resolved imaging of the top face of the particles would be necessary for a more detailed

(24) Szökő, J.; Berkó, A. *Vacuum* **2003**, *71*, 193.

(25) Lai, X.; Guo, Q.; Min, B. K.; Goodman, D. W. *Surf. Sci.* **2001**, *487*, 1.

Table 1. Interpretation of the Various 1D Features Formed on a TiO₂(110) Surface Given in the Literature

light rows of (1 × 1)	5-fold Ti ⁴⁺ rows	refs 18 and 21
light rows of (1 × 2)	regularly grown epitaxial outrising Ti ₂ O ₃ rows	refs 18 and 21
DS on (1 × 2)	antiphase boundaries (APBs) of neighboring (1 × 2) islands	ref 19
DS on (1 × 1)	randomly outrising Ti ₃ O ₅ added rows	ref 22
DS on (1 × 1)	added Ti ₂ O ₃ rows	ref 23
DS on (1 × 1)	missing 5-fold Ti and O rows accompanied by relaxation of the neighboring rows	this work
BS on (1 × 1)	irregular missing bridging O atoms and 6-fold Ti atoms underneath	ref 17
BS on (1 × 1)	randomly outrising Ti ₂ O ₃ rows	ref 22
BS on (1 × 1)	added Ti ₃ O ₅ rows	ref 23
BS on (1 × 1)	randomly O deficient outrising Ti ₃ O ₅	this work

description of the chemical state of the nanoparticles observed in this work.

4. Discussion

4.1. Relevance of the BS and DS Structures in the Formation of Mo Nanoparticles on TiO₂(110). STM results presented in this work have shown that the so-called bright and dark 1D strands (BS, DS) play an important role in the nanostructural properties of the Mo layer, especially at very low coverages. Accordingly, we devote some attention to the identification of these morphological features debated recently by some authors.^{22,23} The series of STM images presented in Figure 1D–I clearly suggest that the shorter bright rows (BS) and the longer dark rows (DS) can be imaged with different contrasts. This behavior can only be explained by the change of the tip atom state and not by the change of the surface or of the imaging parameters. Our data also revealed that the probability of the appearance of the three different contrasts is not equal. The most frequently occurring imaging results in two types of outrising stripes with heights of 0.08 and 0.16 nm, where the height of the rows of the (1 × 1) arrangement is 0.02 nm (Figure 1D,G). These values are somehow smaller than those reported in the earlier papers:^{22,23} 0.15 and 0.26 nm for DS and BS, respectively. In the transition state, the imaging results characteristically in double ridges of both the BS and DS stripes (Figure 1E,H). This latter type of the imaging cannot be stabilized for a longer imaging period of time because it turns easily into the third type of imaging where the longer stripes (DS) appear like black rows of 0.11 nm depth with the same periodicity as the (1 × 1) light rows exhibiting a height of 0.04 nm (Figure 1F,I). This morphology seemingly contradicts somewhat the earlier interpretation of DS structures.²² Takakusagi et al. assigned the DS structures to a more reduced Ti₃O₅ 1D phase with triple ridges found on atomically resolved images. Taking into account our experimental results showing that the light rows ordered to the 5-fold Ti⁴⁺ are somewhat perturbed in the neighborhood of the black rows, we suggest the DS structures may be identified with 1D missing faults of the (1 × 1) bulk-terminated structure (maybe by missing 5-fold Ti⁴⁺ and three neighboring O rows) with some relaxation of the circumvented bridging oxygen atoms. This arrangement gives a slightly oxygen deficient character to this feature. On the basis of the earlier identifications (see above), the BS feature can be attributed to an outrising 1D Ti₃O₅ phase with irregular defects.¹⁷ In Table 1 we collected all the 1D features detected on the TiO₂(110) surface with respect to their morphology and identification given in the different works. From the point of view of the main message of this work, the important statement is that both the DS and BS structures are more reduced sites than the (1 × 1) stoichiometric surface regions.

Mo deposition at low coverage results in an enhanced accumulation of the larger 0D Mo nanoparticles in the regions of both the BS and DS structures, as was imaged

in Figure 3D–F. The appearance of the larger nanoparticles with higher preference in these regions suggests higher diffusion rates of Mo atoms along these structures and in this way a higher accumulation rate into larger particles. In other words, this observation leads to the idea that, for the production of highly dispersed Mo layers, a well-ordered bulk-terminated TiO₂(110)-(1 × 1) surface is necessary. This conclusion seems to be in good harmony with the results presented by Domenichini et al.^{12,14} They concluded that the interface between the Mo layer and the TiO₂(110) support is sharper when the oxide support is stoichiometric and well ordered. Moreover, they have experimentally proved that the role of the deposition rate is also decisive with respect to the quality of the Mo/TiO₂ interface.¹¹ While the larger nanoparticles ($d > 1$ nm) were clearly detectable, the smaller ones containing only a few atoms were difficult to image. The careful evaluation of the ordered (1 × 1) regions in the case of a few percent of Mo coverage has shown, however, that 2D aggregates of a few atoms ($d < 1$ nm) are indeed formed in this region. These aggregates are possibly MoO_x species formed in the reaction of the individual Mo atoms with the bridge oxygen of the substrate. This statement is confirmed by the earlier XPS measurements showing that the TiO₂(110) support became partially reduced already at room temperature after being exposed to Mo.^{9,12} The position of these tiny MoO_x species relative to the bridge oxygen and 5-fold Ti⁴⁺ rows indicates their localization somewhere between the dark and light rows. This configuration means that Mo atoms are coordinated by both the bridging and basal oxygen atoms, resulting in “quasi” oxide species just in the interrow regions of the Ti and O rows of the TiO₂(110) substrate. This observation supports strongly the idea published recently for V deposited on a TiO₂(110) surface.²⁶ With the increase of the Mo coverage up to a few monolayers, a clear 3D growth takes place and the nanoparticles become more metallic as indicated by the STS spectra.

4.2. Thermally Induced Morphological Changes Accompanied by Modification of the Oxidation State. As shown in Figure 5, the morphology of the Mo adlayer deposited at 300 K hardly changes on annealing below 700 K. Both the size and the shape of the nanoparticles, however, change dramatically above this temperature. Especially at high coverages (above 1 ML), it can be seen that the larger particles became rectangular and oriented in both the [001] and [110] directions. The short strings formed in the case of very low Mo coverage are probably reduced Ti₃O₅ stripes, the result of the reordering of the oxygen-deficient surface of the substrate. Nevertheless, it cannot completely be excluded that these 1D structures can be identified with an ordered phase of MoO_x species showing high wetness ability to the support. The high wetness ability of the larger particles at higher coverages is manifested in the anisotropic shape of the particles and their alignment to the support (Figure 5C,D).

(26) Agnoli, S.; Castellarin-Cudia, C.; Sambì, M.; Surnev, S.; Ramsey, M. G.; Granozzi, G.; Netzer, F. P. *Surf. Sci.* **2003**, *546*, 117.

According to the experimental results presented by Domenichini et al.,¹² we may assume that the rectangular nanoparticles formed by annealing in UHV at 900 and 1050 K are Mo(100) grown in the orientation of Mo(100)-[001]/TiO₂(110)[001]. At the same time, our STS measurements performed on the top of the crystallites have shown an increase of the insulator character on thermal treatment. Excluding the complete bulk oxidation of the Mo particles or the formation of an added TiO_x layer on the top of the Mo particles, this latter fact may suggest the formation of an ordered molybdenum oxide interface layer between the support and the Mo nanoparticles. Accepting this mechanism, the sublimation of Mo in the form of MoO₃ species probably takes place at the perimeter sites of the supported nanoparticles, where the oxidation process is limited mainly by the diffusion rate of the bulk oxygen.

5. Conclusions

The TiO₂(110) sample used in this work exhibited characteristically large terraces of (1 × 1) arrangement decorated randomly by two different types of 1D features: shorter (10–20 nm) well outrising strands (BS) and more extended (100–150 nm) less outrising strands (DS). It was shown that Mo nanoparticles of 1–2 nm average diameter formed by the deposition of metal at 300 K. A remarkable site preference was observed: larger Mo nanoparticles are located on the 1D strands (BS, DS). The high dispersity of the Mo layer does not change up to 700 K, which is indicated by the constant particle size in the Mo adlayer. The *I*–*V* curves recorded on the Mo/TiO₂-

(110) samples annealed at temperatures below 700 K indicate clearly the metallic character of the independent nanoparticles. Following annealing up to 900 K, a dramatic change appears both in the morphology and in the spectroscopy of the nanoparticles: they agglomerate readily into larger particles (4–5 nm), and the STS spectra recorded on the top of the particles refer to an insulator character. Depending on the initial metal coverage, the total volume of the adparticles gradually decreases on thermal treatment above 1000 K. A more extended annealing at 1100 K can cause the complete disappearance of the nanoparticles. This behavior may be explained by the volatility of MoO₃ surface species formed at the perimeter of the Mo nanoparticles of Mo(100)[001]/TiO₂(110)[001]. *I*–*V* spectra taken on the particles formed after annealing at 1100 K refer to nanoobjects of a wide band gap (~2.5 eV). This observation may be explained by several possible mechanisms: (i) the complete oxidation of the Mo particles; (ii) formation of a decoration TiO_x layer on the top of the Mo particles; (iii) formation of a well-ordered MoO_x interface between the particles and the support. Taking into account previous data obtained on this material system, the latter mechanism seems to be the most probable.

Acknowledgment. We thank Dr. Albert Oszkó for the careful revision of the manuscript. This work was financially supported by the Hungarian Scientific Research Fund (ÓTKA) through the TS40877, T046351, and T043057 projects.

LA046826M